Research Article | Vol. 24, No. 14 | 11 Jul 2016 | OPTICS EXPRESS 15468

Optics EXPRESS

Role of heat accumulation in the multi-shot damage of silicon irradiated with femtosecond XUV pulses at a 1 MHz repetition rate

RYSZARD SOBIERAJSKI,[1,*] IWANNA JACYNA,[1] PIOTR DŁUŻEWSKI,[1] MARCIN T. KLEPKA,[1] DOROTA KLINGER,[1] JERZY B. PEŁKA,[1] TOMÁŠ BURIAN,[2] VĚRA HÁJKOVÁ,[2] LIBOR JUHA,[2,3] KAREL SAKSL,[2,4] VOJTĚCH VOZDA,[2] IGOR MAKHOTKIN,[5] ERIC LOUIS,[5] BART FAATZ,[6] KAI TIEDTKE,[6] SVEN TOLEIKIS,[6] HARTMUT ENKISCH,[7] MARTIN HERMANN,[7] SEBASTIAN STROBEL,[7] ROLF A. LOCH,[8] AND JAROMIR CHALUPSKY[2]

[1]*Institute of Physics, Polish Academy of Sciences, al. Lotnikow 32/46, 02-668 Warsaw, Poland*
[2]*Institute of Physics, Czech Academy of Sciences, Na Slovance 2, Prague 8, 182 21, Czech Republic*
Institute of Plasma Physics, Czech Academy of Sciences, Za Slovankou 3, Prague 8, 182 00, Czech Republic
[4]*Institute of Materials Research, Slovak Academy of Sciences, 040 01 Kosice, Slovak Republic*
[5]*MESA + Institute for Nanotechnology, University of Twente, The Netherlands*
[6]*DESY, Notkestr. 85, 22607 Hamburg, Germany*
[7]*Carl Zeiss SMT GmbH, Rudolf-Eber-Straße 2, 73447 Oberkochen, Germany*
[8]*Max-Planck-Institut für Struktur und Dynamik der Materie, Luruper Chaussee 149, 22761 Hamburg, Germany*
**ryszard.sobierajski@ifpan.edu.pl*

Abstract: The role played by heat accumulation in multi-shot damage of silicon was studied. Bulk silicon samples were exposed to intense XUV monochromatic radiation of a 13.5 nm wavelength in a series of 400 femtosecond pulses, repeated with a 1 MHz rate (pulse trains) at the FLASH facility in Hamburg. The observed surface morphological and structural modifications are formed as a result of sample surface melting. Modifications are threshold dependent on the mean fluence of the incident pulse train, with all threshold values in the range of approximately 36-40 mJ/cm^2. Experimental data is supported by a theoretical model described by the heat diffusion equation. The threshold for reaching the melting temperature (45 mJ/cm^2) and liquid state (54 mJ/cm^2), estimated from this model, is in accordance with experimental values within measurement error. The model indicates a significant role of heat accumulation in surface modification processes.

© 2016 Optical Society of America

OCIS codes: (140.2600) Free-electron lasers (FELs); (350.1820) Damage; (340.7480) X-rays, soft x-rays, extreme ultraviolet (EUV); (160.6000) Semiconductor materials; (350.3850) Materials processing.

References and links

1. K. Tiedtke, A. Azima, N. von Bargen, L. Bittner, S. Bonfigt, S. Dusterer, B. Faatz, U. Fruhling, M. Gensch, C. Gerth, N. Guerassimova, U. Hahn, T. Hans, M. Hesse, K. Honkavaar, U. Jastrow, P. Juranic, S. Kapitzki, B. Keitel, T. Kracht, M. Kuhlmann, W. B. Li, M. Martins, T. Nunez, E. Plonjes, H. Redlin, E. L. Saldin, E. A. Schneidmiller, J. R. Schneider, S. Schreiber, N. Stojanovic, F. Tavella, S. Toleikis, R. Treusch, H. Weigelt, M. Wellhofer, H. Wabnitz, M. V. Yurkov, and J. Feldhaus, "The soft x-ray free-electron laser FLASH at DESY: beamlines, diagnostics and end-stations," New J. Phys. **11**(2), 023029 (2009).
2. D. Pile, "X-rays: First light from SACLA," Nat. Photonics **5**(8), 456–457 (2011).
3. P. Emma, R. Akre, J. Arthur, R. Bionta, C. Bostedt, J. Bozek, A. Brachmann, P. Bucksbaum, R. Coffee, F. J. Decker, Y. Ding, D. Dowell, S. Edstrom, A. Fisher, J. Frisch, S. Gilevich, J. Hastings, G. Hays, P. Hering, Z. Huang, R. Iverson, H. Loos, M. Messerschmidt, A. Miahnahri, S. Moeller, H. D. Nuhn, G. Pile, D. Ratner, J. Rzepiela, D. Schultz, T. Smith, P. Stefan, H. Tompkins, J. Turner, J. Welch, W. White, J. Wu, G. Yocky, and J. Galayda, "First lasing and operation of an angstrom-wavelength free-electron laser," Nat. Photonics **4**(9), 641–647 (2010).
4. K. Honkavaara, B. Faatz, J. Feldhaus, S. Schreiber, R. Treusch, and M. Vogt, "Status of the sof x-ray user facility FLASH," *Proceedings of FEL2015*, Daejeon, Korea (2015).

#263357 http://dx.doi.org/10.1364/OE.24.015468
Journal © 2016 Received 18 Apr 2016; revised 3 Jun 2016; accepted 3 Jun 2016; published 29 Jun 2016

5. N. Stojanovic, D. von der Linde, K. Sokolowski-Tinten, U. Zastrau, F. Perner, E. Forster, R. Sobierajski, R. Nietubyc, M. Jurek, D. Klinger, J. Pelka, J. Krzywinski, L. Juha, J. Cihelka, A. Velyhan, S. Koptyaev, V. Hajkova, J. Chalupsky, J. Kuba, T. Tschentscher, S. Toleikis, S. Dusterer, and H. Redlin, "Ablation of solids using a femtosecond extreme ultraviolet free electron laser," Appl. Phys. Lett. **89**(24), 241909 (2006).
6. D. W. Bäuerle, *Laser Processing and Chemistry* (Springer Science & Business Media, 2013).
7. J. Krzywinski, R. Sobierajski, M. Jurek, R. Nietubyc, J. B. Pelka, L. Juha, M. Bittner, V. Letal, V. Vorlicek, A. Andrejczuk, J. Feldhaus, B. Keitel, E. L. Saldin, E. A. Schneidmiller, R. Treusch, and M. V. Yurkov, "Conductors, semiconductors, and insulators irradiated with short-wavelength free-electron laser," J. Appl. Phys. **101**(4), 043107 (2007).
8. J. B. Pelka, A. Andrejczuk, H. Reniewicz, N. Schell, J. Krzywinski, R. Sobierajski, A. Wawro, Z. R. Zytkiewicz, D. Klinger, and L. Juha, "Structure modifications in silicon irradiated by ultra-short pulses of XUV free electron laser," J. Alloys Compd. **382**(1-2), 264–270 (2004).
9. S. P. Hau-Riege, R. A. London, R. M. Bionta, M. A. McKernan, S. L. Baker, J. Krzywinski, R. Sobierajski, R. Nietubyc, J. B. Pelka, M. Jurek, L. Juha, J. Chalupsky, J. Cihelka, V. Hajkova, A. Velyhan, J. Krasa, J. Kuba, K. Tiedtke, S. Toleikis, T. Tschentscher, H. Wabnitz, M. Bergh, C. Caleman, K. Sokolowski-Tinten, N. Stojanovic, and U. Zastrau, "Damage threshold of inorganic solids under free-electron-laser irradiation at 32.5 nm wavelength," Appl. Phys. Lett. **90**(17), 173128 (2007).
10. J. B. Pelka, R. Sobierajski, D. Klinger, W. Paszkowicz, J. Krzywinski, M. Jurek, D. Zymierska, A. Wawro, A. Petroutchik, L. Juha, V. Hajkova, J. Cihelka, J. Chalupsky, T. Burian, L. Vysin, S. Toleikis, K. Sokolowski-Tinten, N. Stojanovic, U. Zastrau, R. London, S. Hau-Riege, C. Riekel, R. Davies, M. Burghammer, E. Dynowska, W. Szuszkiewicz, W. Caliebe, and R. Nietubyc, "Damage in solids irradiated by a single shot of XUV free-electron laser: irreversible changes investigated using x-ray microdiffraction, atomic force microscopy and Nomarski optical microscopy," Radiat. Phys. Chem. **78**(10), 546–552 (2009).
11. W. Wierzchowski, K. Wieteska, D. Klinger, R. Sobierajski, J. B. Pelka, D. Żymierska, T. Balcer, J. Chalupský, J. Gaudin, V. Hájková, T. Burian, A. J. Gleeson, L. Juha, H. Sinn, D. Sobota, K. Tiedtke, S. Toleikis, T. Tschentscher, L. Vyšín, H. Wabnitz, and C. Paulmann, "„Investigations of the damages induced by flash pulses in silicon crystals by means of white beam synchrotron section topography," Radiat. Phys. Chem. **93**, 99–103 (2013).
12. T. Koyama, H. Yumoto, Y. Senba, K. Tono, T. Sato, T. Togashi, Y. Inubushi, J. Kim, T. Kimura, S. Matsuyama, H. Mimura, M. Yabashi, K. Yamauchi, H. Ohashi, and T. Ishikawa, "Damage study of optical substrates using 1-µm-focusing beam of hard x-ray free-electron laser," J. Phys. Conf. Ser. **463**, 012043 (2013).
13. T. Koyama, H. Yumoto, Y. Senba, K. Tono, T. Sato, T. Togashi, Y. Inubushi, T. Katayama, J. Kim, S. Matsuyama, H. Mimura, M. Yabashi, K. Yamauchi, H. Ohashi, and T. Ishikawa, "Investigation of ablation thresholds of optical materials using 1-µm-focusing beam at hard X-ray free electron laser," Opt. Express **21**(13), 15382–15388 (2013).
14. S. P. Hau-Riege, H. N. Chapman, J. Krzywinski, R. Sobierajski, S. Bajt, R. A. London, M. Bergh, C. Caleman, R. Nietubyc, L. Juha, J. Kuba, E. Spiller, S. Baker, R. Bionta, K. Sokolowski Tinten, N. Stojanovic, B. Kjornrattanawanich, E. Gullikson, E. Plönjes, S. Toleikis, and T. Tschentscher, "Subnanometer-scale measurements of the interaction of ultrafast soft x-ray free-electron-laser pulses with matter," Phys. Rev. Lett. **98**(14), 145502 (2007).
15. A. R. Khorsand, R. Sobierajski, E. Louis, S. Bruijn, E. D. van Hattum, R. W. E. van de Kruijs, M. Jurek, D. Klinger, J. B. Pelka, L. Juha, T. Burian, J. Chalupsky, J. Cihelka, V. Hajkova, L. Vysin, U. Jastrow, N. Stojanovic, S. Toleikis, H. Wabnitz, K. Tiedtke, K. Sokolowski-Tinten, U. Shymanovich, J. Krzywinski, S. Hau-Riege, R. London, A. Gleeson, E. M. Gullikson, and F. Bijkerk, "Single shot damage mechanism of Mo/Si multilayer optics under intense pulsed XUV-exposure," Opt. Express **18**(2), 700–712 (2010).
16. R. Sobierajski, M. Jurek, J. Chalupsky, J. Krzywinski, T. Burian, S. D. Farahani, V. Hajkova, M. Harmand, L. Juha, D. Klinger, R. A. Loch, C. Ozkan, J. B. Pelka, K. Sokolowski-Tinten, H. Sinn, S. Toleikis, K. Tiedtke, T. Tschentscher, H. Wabnitz, and J. Gaudin, "Experimental set-up and procedures for the investigation of XUV free electron laser interactions with solids," J. Instrum. **8**(02), 013909 (2013).
17. K. Tiedtke, J. Feldhaus, U. Hahn, U. Jastrow, T. Nunez, T. Tschentscher, S. Bobashev, A. Sorokin, J. Hastings, S. Möller, L. Cibik, A. Gottwald, A. Hoehl, U. Kroth, M. Krumrey, H. Schöppe, G. Ulm, and M. Richter, "Gas detectors for x-ray lasers," J. Appl. Phys. **103**(9), 094511 (2008).
18. R. Sobierajski, D. Klinger, M. Jurek, J. B. Pelka, L. Juha, J. Chalupský, J. Cihelka, V. Hajkova, L. Vysin, U. Jastrow, N. Stojanovic, S. Toleikis, H. Wabnitz, J. Krzywinski, S. P. Hau-Riege, and R. London, "Interaction of intense ultrashort XUV pulses with silicon," Proc. SPIE **7361**, 736107 (2009).
19. J. M. Liu, "Simple technique for measurements of pulsed Gaussian-beam spot sizes," Opt. Lett. **7**(5), 196–198 (1982).
20. N. Medvedev, Z. Li, and B. Ziaja, "Thermal and nonthermal melting of silicon under femtosecond x-ray irradiation," Phys. Rev. B **91**(5), 054113 (2015).
21. H. Hu and S. A. Argyropoulos, "Mathematical modelling of solidification and melting: a review," Model. Simul. Mater. Sc. **4**(4), 371–396 (1996).
22. Material's thermodynamical parameterters taken from NIST Chemistry WebBook, *http://webbook.nist.gov/chemistry/*.
23. H. Shanks, P. Maycock, P. Sidles, and G. Danielson, "Thermal conductivity of silicon from 300 to 1400 K," Phys. Rev. **130**(5), 1743–1748 (1963).

Optics EXPRESS

24. B. L. Henke, E. M. Gullikson, and J. C. Davis, "X-ray interactions: photoabsorption, scattering, transmission, and reflection at E= 50-30,000 eV, Z= 1-92," Atom. Data Nucl. Data **54**, 181–342 (1993).
25. A. Rämer, O. Osmani, and B. Rethfeld, "Laser damage in silicon: energy absorption, relaxation, and transport," J. Appl. Phys. **116**(5), 053508 (2014).

1. Introduction

The rapid development of Free Electron Lasers (FELs) operating in the extreme ultraviolet (XUV) and X-ray regions has opened up unprecedented opportunities for generating high energy density states of matter. FELs [1–3] provide quasi-monochromatic and extremely intense pulses of radiation. This enables an extension of studies of radiation induced phase transitions of solids beyond the optical wavelength range, to much shorter wavelengths. Pulse length emitted by FELs is in the order of femtoseconds, much shorter than typical time constants related to structural transformations and to energy transfer processes. It is thus feasible to explore the dynamics of these processes separate from rapid radiation absorption. This dramatically simplifies modelling of subsequent physical processes. Photon pulses can be applied individually or in series (trains) with a repetition rate up to the megahertz range. FEL sources based on superconducting accelerating technology are especially suitable for multi-shot mode operation, in which the sample is exposed to a number of pulses on the same spot. For example, FLASH, a superconducting FEL in Hamburg [4], provides up to 800 XUV pulses of 10-100 fs each with a 1 MHz repetition rate. The pulse spacing of 1 μs is of the order of the typical time constant of heat dissipation from the solid sample surface to the bulk and is therefore suitable for studying heat accumulation processes. Multi-shot excitation of solid materials with soft X-ray pulses offers a number of advantages over irradiation with sources operating in the optical range. First of all, the energy deposition process is practically undisturbed by optical nonlinearities caused by processes such as multiphoton and free carrier absorption. Moreover, the absorption depth can be controlled, over orders of magnitude, by tuning the FEL to an appropriate wavelength (e.g. just above the absorption edge). Thus, ultrashort XUV pulses provide a method to create well-defined excitation conditions in a large sample volume [5]. In such a case temperature gradients are low and the influence of the heat dissipation processes is sustained. Using FELs, it becomes possible to significantly extend the optical studies of phase transitions by systematic studies of transition dynamics, energy transfer, and accumulation processes.

Among the many materials studied regarding their structural modifications and damage, silicon plays a significant role, since it is treated as a reference material (it is relatively easily accessible and its physical properties are well known) and due to its fundamental importance for electronics and optics. A lot of work on this subject has been carried out using a wide range of optical lasers with different emission characteristics, wavelength (from microwaves to VUV), pulse width (from microseconds to femtoseconds, and CW), repetition rate, and intensity (see [6] for review). For silicon, phase transition mechanisms induced with a single femtosecond and monochromatic pulse of wavelength in the range of XUV and X-ray were studied previously, mainly with an angle of incidence close to surface normal. Bulk crystals [5, 7–13] together with a-Si layers in Si/C and Mo/Si multilayer systems [14, 15] have been examined. These measurements have shown that single shot structural modifications are caused by melting. In this paper we extend the studies of the phase transitions in silicon, induced by femtosecond XUV pulses, to the multi-shot mode with a 1 MHz repetition rate, to investigate cumulative effects.

2. Experiment

A bulk, (001)-oriented, silicon single crystal with a super-polished top surface was used in this study. The sample was found to have a surface roughness less than 0.2 nm (RMS) measured by X-ray reflectometry and atomic force microscopy. The sample size was 10x40 mm^2 with a thickness of 900 μm. The experiment was conducted at the BL2 beamline at the

FLASH facility [1] in an ultrahigh vacuum (at a 10^{-7} mbar pressure level) chamber using standard methods and experimental techniques for FEL damage studies described in [16]. Samples were exposed to femtosecond XUV radiation, with the wavelength centred at 13.5 nm and a bandwidth of 1% (FWHM). The incidence angle was 15.5 degrees off normal. Pulse duration, estimated from electron bunch charge, was approximately 100 fs (FWHM). Each irradiated spot accumulated a train of 400 single pulses with a 1 MHz repetition rate. Pulse energies were recorded for each shot by means of a gas monitor detector [17]. Pulse energy distributions for various spots, normalized to the mean pulse train energy are presented in Fig. 1. Pulse energies for a given spot varied from a trend line by approximately ± 20%. Total variation of the energy at each spot was approximately ± 40%. Gas and solid attenuators were used to control the mean energy of pulse trains for each spot. The maximum beam fluence at the irradiation position was reduced to 64 mJ/cm^2 – i.e. well below the single-pulse surface modification threshold fluence (approximately 410 mJ/cm^2). Therefore avoiding mixing of single and multi-shot irradiation conditions, which could influence the path of the structural modification. Measurements were performed with the sample placed out of focus of the ellipsoidal mirror. The spot effective area was about 91 000 μm^2. Two apertures of 5 and 3 mm separated by a 5 m distance were used to control the direction of the beam propagation to minimize variations of the spot position on the sample.

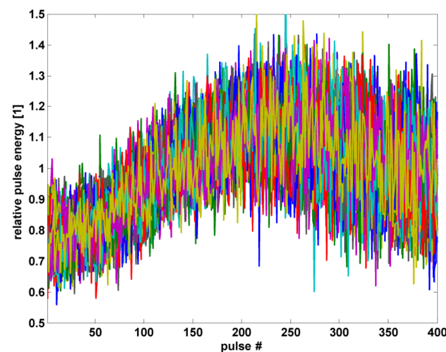

Fig. 1. Pulse energy distributions for various spots (different colours on the plot) normalized to the mean train energy.

After irradiation spots were investigated by optical microscopy with differential interference contrast (DIC) using a Nomarski prism, sensitive to changes of morphology and optical properties of the material (Fig. 2(a)); and scanning electron microscopy (SEM) mapping the surface's morphology (Fig. 2(b)). Sample cross-sections at selected positions inside the irradiated spot were studied by means of transmission electron microscopy (TEM). In Fig. 2 three different regions can be distinguished. The outer region, with the largest area, can be distinguished by a different contrast in the DIC microscope image. The SEM image shows that the surface in this region is partially covered with nanodroplets, with a 30-50 nm diameter, separated by approximately 100-150 nm. Such droplets can also be seen in the TEM images (see Fig. 3(a)). They seem to be epitaxially grown crystallites. Below some of these crystals is a volume with a large number of crystal defects. The characteristic feature of the middle region is a very rough surface (see Fig. 2). SEM images and TEM cross-sections reveal that the surface morphology is dominated by droplets, similar to those observed in the first region, but located much closer to each other. A continuous layer comprising of a dense network of lattice defects extends just beneath the sample surface to a depth of about 0.5 μm (see Fig. 3(b)). Such defect structures, but of much lower density, can be observed in deeper parts of the sample over the whole depth of the 4 μm cross-section. The inner region has a smooth surface which seems to be formed (as a bulge or a crater with a wall-type embankment) by hydrodynamic processes (e.g. material expansion or lateral movement) and

resembles those observed in silicon samples irradiated with XUV radiation of 13.5 nm wavelength at normal incidence, with a fluence above the single shot damage threshold [18]. TEM images in this region reveal fewer defects in the surface vicinity, than in the middle region (Fig. 3(c)). All three final states of the sample occur only if the mean local radiation fluence exceeds the thresholds values. Based on the DIC images of irradiated spots, threshold values were established by means of the Liu's method taking into account these 3 different criteria of damage [16, 19]. Values are very close to each other: 38 mJ/cm^2 for the outer, 40 mJ/cm^2 for the middle, and 42 mJ/cm^2 for the inner region, with a relative experimental error of approximately ± 20%.

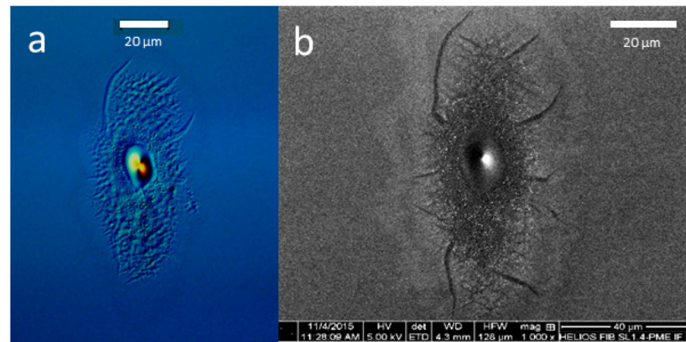

Fig. 2. DIC optical microscopy (a) and SEM (b) images of a spot irradiated at a fluence level of 42.5 mJ/cm^2.

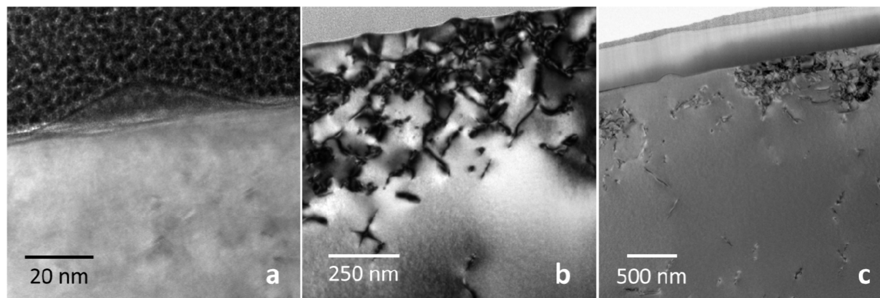

Fig. 3. TEM images of sample cross-sections taken at the spot presented on Fig. 2 in three areas: (a) droplet–like surface feature of the outer region, (b) 0.5 µm thick layer of lattice defects in the vicinity of the sample surface in the middle region, (c) lattice defects at the border between the middle and inner regions. A polycrystalline ultrathin Pt cap layer is visible on top of the sample. It was deposited for sample protection during cross-sectional cutting using focus ion beam (FIB). FIB processing was carried out after irradiation and measurement with DIC optical microscopy and SEM.

For comparison, reference silicon samples were irradiated with 4000 and 400 pulses at a 10 Hz repetition rate (accumulated single pulses instead of pulse trains). The mean fluence of accumulated pulses at the irradiation position was up to 43 mJ/cm^2, a higher value than the surface modification threshold for a 1 MHz repetition rate. In this case, no surface modifications in the exposed spots were observed by means of DIC microscopy.

The single shot melting threshold was not directly determined for irradiation at a 13.5 nm wavelength at normal incidence. Instead, it was estimated to be 410 mJ/cm^2, from experimental values obtained for irradiations at the wavelength of 32.5 nm [5, 9] and 0.124 nm (10 keV photon energy) [12, 13] and theoretical predictions [20].

Optics EXPRESS

3. Simulations

Heat accumulation and transport was simulated by means of a simple 1-D heat diffusion model. The problem was solved using the enthalpy method [21] in which evolution of latent heat was accounted for by enthalpy as well as the relationship between enthalpy and temperature. A simple 1-D geometry of the sample, where the temperature and enthalpy is uniform over planes parallel to the sample surface and varies only in the perpendicular direction (in depth), was used. This is justified by the fact that the effective XUV beam spot diameter during the experiment was in the order of 300 μm, and therefore all temperature gradients were much smaller in the lateral direction than in-depth. In this case, heat diffusion can be expressed by the following equation:

$$\frac{\partial h}{\partial t} = \frac{\partial}{\partial x}\left(\frac{k}{C}\frac{\partial h}{\partial x}\right) + S, \tag{1}$$

where h is the local enthalpy of the sample expressed in [J/m^3] depending on spatial (x [m]) and time (t [s]) variables, k is the total (sum of electron and phonon) heat conductivity expressed in [W/(mK)], C is heat capacity expressed in [J/(Km^3)], and S is the source term with units of [W/m^3]. The relationship between enthalpy and temperature was found in [22], while the k/C ratio dependence on enthalpy was calculated based on data provided in [23]. The enthalpy scale can be divided into three regions: for h lower than approximately 3 GJ/m^3 when the temperature stays below the melting temperature T_{melt} = *1683 K*, h between approximately 3 and 7.17 GJ/m^3, when the temperature stays constant at the T_{melt} for all enthalpy values, and for h above 7.17 GJ/m^3, when sample is in liquid form (change into gas phase was not considered in the current studies). When the temperature is equal to T_{melt}, heat capacity tends to infinity (as temperature remains constant when heat is added to the system) and k/C is equal to zero.

The source term, S, corresponds to the absorption of radiation. Its depth dependence is proportional to the exponential absorption term ~exp($-x/L_{abs}$) following Lambert-Beer's law with L_{abs} equal to 568.5 nm (radiation penetration depth at a 13.5 nm wavelength and incidence angle of 15.5°, based on [24]). Sample thickness was taken in the calculations as 900 μm. It was assumed that there is no heat transfer at the sample boundaries. The observed temperature rise on the back of the sample surface was less than 1 K for all simulations. The initial value of enthalpy in the sample was taken as zero ($h(x)$ = 0 for all x), and the temperature of the sample as 298 K. Although the pulse duration was approximately 100 fs, the time scale of the source term (modelled by one period of a sin^2 function) was set to 2 ps. This corresponds to the characteristic electron-phonon coupling time constant representing the time needed to transfer energy absorbed by electrons to the lattice [25]. The maximum power density of the source term (p) is a function of the radiation fluence (F), sample reflectivity ($R \approx 0$), and L_{abs}: $p = (1-R)*F/L_{abs}$. Due to relatively small temperature gradients in the investigated system, determined mostly by the radiation penetration depth, energy diffusion by electron gas before thermalization with the lattice was neglected. Multi-shot irradiations were calculated in the following sequence. First, the heat equation was solved for a 1 μs period, i.e. the time between successive laser pulses. Next, the final state of calculations for the first pulse was taken as an initial state for the second pulse. This was exactly repeated in 1 μs steps for the given number of pulses. The estimated relative error of simulations are approximately 20% and are associated with the above discussed approximations (1-D geometry, choice of the source term etc.) and the accuracy of the chosen model parameters (such as heat conductivity dependency on the enthalpy).

Analysis of the theoretical model started with calculations of the enthalpy depth distribution variability up to 1 μs after the absorption of a single XUV pulse. An example result for a fluence of 500 mJ/cm^2 is shown in Fig. 4. The maximum enthalpy on the top sample surface was calculated for various fluence levels over the range of 0.5 - 500 mJ/cm^2.

Optics EXPRESS

Threshold values of 3 and 7.17 GJ/m^3 are reached at the surface for fluences of 170 and 410 mJ/cm^2, respectively. Based on these simulations and experimental data for other wavelengths in the XUV range [5, 9], the single shot melting threshold was estimated to be approximately 410 mJ/cm^2. Furthermore, an increase in the residual enthalpy at the top sample surface after a calculation time step of 1 μs was obtained. The calculation shows that, when the next pulse should arrive, there is still a significant fraction of heat left at the sample surface by the preceding pulse, so heat accumulation must take place in the multi-shot case.

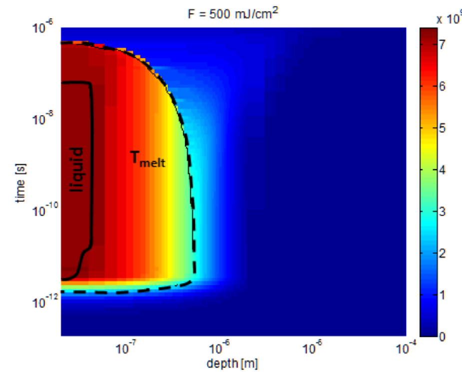

Fig. 4. Simulation's result for a fluence of 500 mJ/cm2. Local enthalpy dependence on time (up to 1 μs) and depth (down to 100 μm). Two enthalpy levels of 3 and 7.17 GJ/m3 corresponding to T = T_{melt} and start of liquid phase are marked with black lines (dashed and solid, respectively). Colour bar values on the right are in [J/m3].

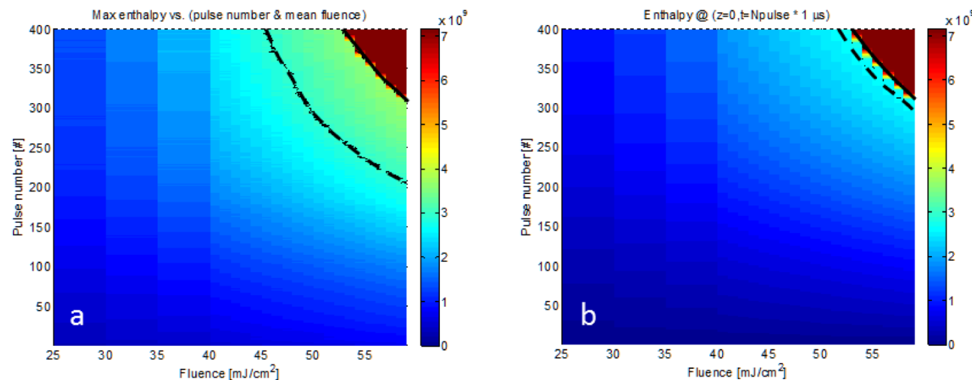

Fig. 5. Maximum enthalpy during each pulse (a) and accumulated enthalpy before each pulse (b) for various mean fluence levels. Two enthalpy levels of 3.0 and 7.17 GJ/m^3 corresponding to T = T_{melt} and the start of liquid phase are marked with black lines (dashed and solid, respectively). The colour map corresponds to an enthalpy range of 0 to 7.17 GJ/m^3 (liquid sample).

Further simulations for 400 pulses at a 1 MHz repetition rate were performed for fluences in the range of 25 to 60 mJ/cm^2. The distribution of pulse energies over the pulse train, equal to the mean pulse energy distribution measured in the experiment (see Fig. 1) was used. Maximum enthalpy during each pulse and accumulated enthalpy before each following pulse for various mean fluence levels is presented in Fig. 5(a) and 5(b), respectively. Two thresholds are marked with black lines - reaching the melting temperature at 3 GJ/m^3 and for the liquid phase at 7.17 GJ/m^3. In Fig. 6 the maximum melting depth after each pulse, for various fluence levels is presented. For enthalpies from 3 up to 7.17 GJ/m^3 (between dashed and solid black lines on Fig. 5(a)), the depth over which samples reach the melting

Optics EXPRESS

temperature, is up to 0.6 μm. This volume increases with increasing fluence and pulse quantity.

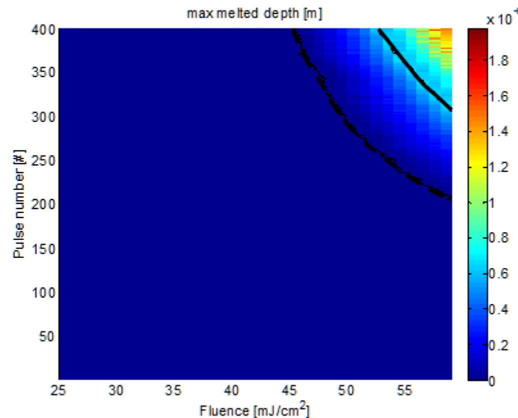

Fig. 6. Map of maximum melted depth after each pulse for various fluence levels. Two enthalpy levels of 3 and 7.17 GJ/m3 corresponding to T = T_{melt} and the start of the liquid phase are marked with black lines (dashed and solid, respectively). The colour map corresponds to a depth range of 0 to 2 μm.

4. Discussion

Three types of surface morphological and structural modifications were observed in silicon samples irradiated with 400 XUV pulses of approximately 100 femtosecond duration at a 1 MHz repetition rate. These modifications evidence a threshold dependency on the mean fluence of the incident pulse train. Above the lowest threshold of 38 mJ/cm^2, only surface changes in a form of nano-droplets can be observed. Our observations suggest that they are formed due to reassembly of a locally molten surface material. Melting occurs only at the sample surface (top few nanometers) and has a lower fluence threshold than that for melting of a bulk material. It may be explained by a lower melting threshold (in terms of enthalpy) of the surface material than the bulk. This depends on surface structural parameters which are related to the sample's surface polishing. The second threshold of 40 mJ/cm^2 is related to formation of a large number of lattice defects in a layer thickness of approximately 0.5 μm. Such behaviour might be explained by enhanced lattice elasticity when the temperature reaches the melting point. Under such conditions, lattice atoms start to dislocate due to thermal movements and broken bonds. As soon as the sample cools down, defects get frozen and stay localized. This process is repeated many times and the number of dislocations grows with the number of irradiating pulses. There are much fewer defects above the third threshold of 42 mJ/cm^2. Under these conditions the sample reaches the liquid (amorphous) phase at the end of the pulse train. The morphology of the central part of the spot can be explained by hydrodynamical movement of the liquid material. Freezing takes time long enough so that a crystalline structure is formed in a quasi-epitaxial process. Some of the dislocations are still frozen but their density is much smaller than dislocations observed originating from the non-liquid state.

The above proposed explanation of the experimental results is supported by the theoretical model described by the heat diffusion equation. Thresholds for reaching the melting temperature (45 mJ/cm^2) and liquid state (54 mJ/cm^2) obtained in simulations are close to, and indeed overlap with experimental values, within the error bounds. Simulations show that as soon as the melting temperature is reached, heat dissipation from the surface slows down abruptly (due to the lack of a temperature gradient at these conditions). Most of the energy of the pulses absorbed after reaching T_{melt} do not diffuse from the surface and adds to the latent

heat of melting at the constant melting temperature. Consequently, thresholds for reaching T_{melt} and the full liquid state are very close to each other, which was observed experimentally.

The model supports the explanation of a high density of defects in the top 0.5 μm layer of samples for fluences above the second threshold fluence. In Fig. 6 it is shown that over a similar depth sample reaches the melting temperature but is not yet liquid. Above the second fluence threshold but below the third one the sample reaches the melting temperature (due to a next pulse absorption) and cools down to below it (due to a heat diffusion) for up to ~150 times. Since the defect formation is not reversed by epitaxial growth from the liquid phase, the defect density increases after each pulse.

No surface damage was observed for multi-pulse irradiations with a 10 Hz repetition rate, when the system has enough time (100 ms) for relaxation between pulses. It indicates that heat accumulation plays an important role in the studied processes. If the delay between subsequent pulses is short enough (in our case, 1 μm) then there is not enough time for complete heat dissipation from the surface, therefore, as a result, the heat accumulates.

In our studies we have neglected the role of the non-thermal melting. The required excitation of the electron gas is much higher than for thermal process (2.0 and 0.7 eV/atom, respectively [20]). In the presented case the accumulation of heat occurs at hundreds of μs, therefore electrons and the lattice are in thermal equilibrium for most of the time. Since the heat capacity of the lattice is higher than the electron gas in the studied temperature range, most of the absorbed energy is stored by phonons. Thus the excitation of the electron gas for a given fluence range is never high enough to trigger the pure non-thermal melting process. However, we cannot exclude a phase transition of a mixed nature resulting from an interplay of thermal and non-thermal processes [20]. Its threshold estimated in simulations (0.9 eV/atom for single femtosecond x-ray pulse) is close to the threshold for thermal melting and could have been reached during irradiations. Since, what we experimentally observe is the final state of the sample after resolidification, we are not able to distinguish the purely thermal process from the mixed one.

5. Summary

The role of heat accumulation on multi-shot damage of silicon was studied. Bulk silicon samples were exposed to 400 intense XUV (wavelength of 13.5 nm) femtosecond pulses at a 1 MHz repetition rate at the FLASH facility in Hamburg. The application of XUV radiation ensured the avoidance of optical nonlinearities, such as multi-photon absorption, and allowed excitation of a relatively large volume of material, up to a depth of approximately 0.5 μm. Three types of surface morphological and structural modifications were observed. They are threshold dependent on the mean fluence of the incident pulse train, with threshold values very close to each other, in the range of approximately 38-42 mJ/cm^2. The observed structures are related to the melting of the sample's surface. The onset of the surface modifications can be observed for radiation fluences approximately 10 times lower than in a single pulse case, which corresponds to an approximately 40 times larger total deposited dose. Experimental data is supported by a theoretical model described by the heat diffusion equation. The threshold for reaching the melting temperature (45 mJ/cm^2) and liquid state (54 mJ/cm^2) obtained in simulations overlap with the experimental values within error bars (20% for the simulated values and 20% for the experimental results). The theoretical model indicates a significant role for heat accumulation on surface modification processes. In the case of a 1 μs delay between subsequent pulses, a significant amount of single pulse energy stays at the sample's surface until the next pulse, in spite of heat diffusion. The accumulated heat leads to lowering of the surface modification threshold.

The studies of the multi-shot accumulation processes in silicon are also of practical importance. Apart from new experimental opportunities, the use of an intense FEL beam creates extreme demands for optics and detectors, primarily on radiation hardness. The presented research helps to specify limits on the use of silicon for new short wavelength FEL

sources e.g. geometrical constraints and structural requirements for optical substrates or front-end elements of detectors.

Acknowledgments

Support from the operators of the FLASH facility is gratefully acknowledged. This work has been partially supported by the Polish National Science Center (Grant No. DEC-2011/03/B/ST3/02453 and DEC-2012/06/M/ST3/00475), the Czech Science Foundation (Grant No. 14-29772S), the Ministry of Education, Youth and Sports of the Czech Republic (Grant No. LH14072) and the Dutch Topconsortia Kennis en Innovatie (TKI) program on high-tech systems and materials (Grant 14 HTSM 05). Furthermore we acknowledge the support of the Industrial Focus Group XUV Optics of the MESA + Institute for Nanotechnolgy of the University of Twente, notably the industrial partners ASML, Carl Zeiss SMT GmbH, PANalytical, SolMates, TNO, and Demcon, as well as the Province of Overijssel and the Foundation FOM.